analytical chemistry

Article

pubs.acs.org/ac

Nanochannel pH Gradient Electrofocusing of Proteins

Michael A. Startsev,*[,†] David W. Inglis,[‡] Mark S. Baker,[§] and Ewa M. Goldys[†]

[†]Department of Physics and Astronomy, Macquarie University, Sydney NSW 2109, Australia

[‡]Department of Engineering, Macquarie University, Sydney NSW 2109, Australia

[§]Department of Chemistry and Biomolecular Sciences, Macquarie University, Sydney NSW 2109, Australia

ABSTRACT: We demonstrate matrix-free pH gradient electrofocusing of proteins within an 85 nm deep nanochannel. In contrast to conventional isoelectric focusing where the fluid does not move, this pH gradient method traps protein molecules flowing through a channel by balancing electric forces due to pH-dependent protein charge and viscous drag forces caused by electro-osmosis. The nanoscale depth of the device and the low voltage used limit convection relative to diffusion, thus producing a stable focused band of protein. R-Phycoerythrin (RPE) and Dylight labeled streptavidin (Dyl-Strep) were focused within a nanochannel using applied voltages between 0.4 and 1.6 V. Concentration enhancement factors of over 380 have been achieved within 5 min. Varying the buffer pH (between 2.7 and 7.2) at the boundaries of the nanochannel affected the shape of the focused bands. For RPE, a pH span of 4.5 (pH 2.7 to 7.2) yielded the narrowest peak while a span of 2.4 (pH 2.7 to 5.1) produced a significantly wider peak. Such matrix-free nanofluidic devices with pH gradient electrofocusing may enable on-chip integration of orthogonal separation techniques with mass spectrometry offering labor savings and enhanced performance.

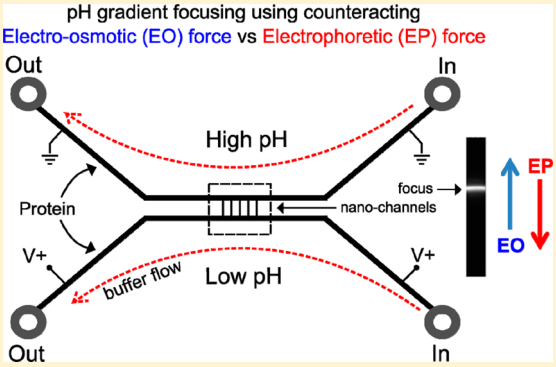

Analytical chemistry techniques such as capillary zone electrophoresis (CZE),[1] 2D gel electrophoresis,[2] high−performance liquid chromatography (HPLC),[3,4] enzyme linked immunosorbent assay (ELISA)[5] and mass spectrometry (MS)[6] are fundamental to proteomic research. A range of counter flow gradient methods have been developed for focusing and separating molecules, and some of these have been used with mass spectrometry in so-called orthogonal separations. Isotachophoresis (ITP)[7,8] and gradient elution moving boundary electrophoresis (GEMBE)[9,10] are two examples of methods of electrokinetic protein focusing and separation methods involving moving focus bands while methods such as capillary isoelectric focusing (cIEF)[11] produce constant focus positions. Our approach is a counter flow gradient method as it employs bulk flow to counteract a gradient in analyte velocity to produce a stationary equilibrium focus position. Ion concentration polarization (ICP)[12−14] has been observed in devices similar to the device used in this work and yielded high preconcentration enhancement factors near the entrances of the micro−nanochannel junctions. However, preconcentration using this technique is limited as its capacity for separation has not been demonstrated. Common types of counter-flow gradient methods are conductivity gradients,[15] chromatographic velocity gradients (counteracting chromatographic electrophoresis or (CACE)[16,17]), current gradients (electric field gradient focusing (EFGF)[18,19]), the electrode array technique,[20] temperature gradient focusing,[21,22] and finally, the method of interest in this work, pH gradients.

Early attempts at protein focusing based on pH gradient principles involved containing acidic and alkaline solutions, respectively, at the anode and cathode of a fluid channel device and inducing a voltage difference at the electrodes.[23] A major drawback of this technique was that the pH gradients formed by the buffers were impossible to stabilize over the time required for focusing, and the ongoing migration of buffer and titrant ions was responsible for the destruction of electrophoretic focus.[24] The problems with stability of the pH gradients were largely overcome by the introduction of immobilized pH gradient polyacrylamide "gels" and ampholytes used within a dispersion medium which are able to maintain a stationary pH gradation under the influence of an electric field. This stability facilitated current isoelectric focusing techniques which are consistent and accurate enough for commercial applications and later enabled the development of the 2D electrophoresis.[2] However, isoelectric focusing and pH gradient techniques are not routinely coupled directly to mass spectrometry in part because the carrier ampholytes which establish the pH gradient negatively affect MS performance. Selective downstream analysis has been demonstrated before by Chingin et al.,[25] this method involved multiple buffer and electrode junctions to trap and release focus bands with a high degree of control.

In this study, we demonstrate matrix-free pH gradient focusing, a novel approach to protein focusing that also presents a promising potential application for on-chip protein separations. A pH gradient exists along a nanofluidic channel

Received: March 5, 2013
Accepted: July 2, 2013
Published: July 2, 2013

   dx.doi.org/10.1021/ac4014447 | *Anal. Chem.* 2013, 85, 7133−7138

connecting two reservoirs of different pH. An electric field applied across the channel exploits the inherent pH-dependent charge properties of proteins in concert with counteracting electro-osmotic (EO) flow such that the proteins become immobilized at an equilibrium position along the channel. We investigate this phenomenon using a naturally fluorescent protein, R-Phycoerythrin (RPE) and Dylight labeled streptavidin (Dyl-Strep). Unlike most other electrophoretic concentration enhancement methods,[26,27] this approach works with a continual supply of protein sample and buffer, so that it may be possible to eventually trap a detectable amount of low abundance molecules. This is in contrast to conventional techniques such as capillary electrophoresis that use a single sample injection at the start of the experiment. Such methods are limited to focusing only the quantity of molecules within the initial injection volume[28] which may be insufficient for the detection of low abundance molecules.

Explanation of the Concentration Mechanism. The electrokinetic forces that govern flow within a nanofluidic channel result from the inherent charge separation phenomena at solid−liquid interfaces. The silanol groups[29] bound to the fused-silica surface of the channel in contact with an aqueous solution experience a pH-dependent deprotonation which results in a bound surface charge. This, in turn, produces the electric double layer (EDL),[30] a mobile ion distribution near the silica surface. When an electric field is applied along the walls of this channel, the mobile ions in the EDL experience an electric force and move, resulting in EO flow. In conditions where the Debye length is small compared with the diameter of the channel, the Helmholtz-Smoluchowski equation predicts a "plug-like" velocity profile of the EO flow with the velocity V_{HS}[30] given by

$$V_{HS} = \frac{\varepsilon_r \varepsilon_o \zeta E}{\eta} \tag{1}$$

Here, E is the local electric field, η is the viscosity of the buffer solution, ε_r is the permittivity of the medium, ε_o is the permittivity of free space, and ζ is the zeta potential of the channel surface. In our case, ζ changes along the length of the channel due to the pH gradient applied. However, the total fluid flow at the input and output must be the same since the aqueous solution is an incompressible fluid. This results in frustrated flow within the channel,[30] a condition where the fluid velocity vector at a certain position along the depth of the channel can be oriented opposite to the bulk flow. The significance of the frustrated flow relative to the diffusion is captured by the Peclet number (Pe_L):[31]

$$Pe_L = \frac{LU}{D} \tag{2}$$

where U is the particle transport speed, L is the characteristic length (85 nm), and the D is the diffusion coefficient. For the low voltages used here, we observe transport speeds along the length of the channel of less than 50 μm/s, giving a Pe_L number of less than 0.2. This implies that the protein molecules diffuse quickly across the channel depth compared with the EO fluid velocity, averaging the flow profile and allowing us to use a one-dimensional approach where we assume that the EO fluid velocity and force on the protein molecules are independent of the position within the channel. This EO flow exerts a force on the protein. In the case of proteins with a quasi-spherical conformation, in which a represents the effective radius of the spherical protein molecule, this force can be approximated as follows:[32]

$$F_{EO} = 6\pi\eta a V_{HS} \tag{3}$$

The second significant force on the protein is the electrophoretic (EP) force which can be similarly approximated as a Coulomb force on a point charge:

$$F_{EP} = qE \tag{4}$$

where q is the effective charge of the protein at the pH it experiences in the channel. In this study, q is the parameter that varies with pH along the channel. At a certain position within the channel, the protein acquires a value of charge q so that the EP and EO forces balance. In this case, the net drift velocity of the protein becomes zero, and thus, a protein focus band will form at that position. In this simplified 1D case, focusing takes place when the total force, $F = 6\pi\eta a V_{HS} + qE$, is zero. Additionally, to achieve a stable focus, the derivative of the force at the focus point must be negative; i.e., the EO and EP forces on either side of the net zero velocity point must be oriented toward the focus point.

Figure 1a illustrates the effect of combined electrokinetic forces on a protein. In this example, an electric field applied axially along the length of the channel induces an EO force on the "sheath" of positive charges along the walls of the channel in the direction of the electric field. Simultaneously, the electric field also applies a counteracting EP force on the protein (blue sphere) proportional to the instantaneous negative charge of the protein. As suggested by Figure 1b, the protein charge decreases as pH increases. Within the channel, the protein reaches a position where the protein charge-dependent EP force is equivalent to the counteracting EO force as shown by the intersection of red and blue lines in Figure 1c. At this position, the protein becomes immobilized. If the protein moves away from the focus position by means of diffusion, the charge of the protein will change again (due to altered pH) and the net electrokinetic force will become nonzero in the direction toward the focus point. The protein is thus "trapped" at the electrokinetic focus point which, unlike in standard isoelectric focusing, is not a zero charge point of the protein under consideration but the point where EO and EP forces balance.

METHODOLOGY

Fabrication. The nanochannel device shown by the top-view schematic in Figure 2 was fabricated using standard techniques. The microchannels were photolithographically patterned using SU-8 photoresist and etched by deep reactive ion etching at the Australian National Fabrication Facility at the University of South Australia to a depth of 12.5 ± 0.5 μm. The SU-8 was removed by baking in air at 900 °C for 5 h. A variety of tapered and rectangular nanochannels connecting the microchannels were patterned by a second round of photolithography using AZ-1518 photoresist (Microchem, MA, USA). Note that only the rectangular nanochannels are studied here. Nanochannels were etched in a CF4 plasma (9% of 250 sccm CF4, 2% of 100 sccm O2, 150W) in a March PX-250 plasma asher for a total of 12 min to a depth D = 85 ± 5 nm. The nanochannels were patterned to have a length L = 100 μm and a width W = 20 μm. After the etch process, through-holes were created at the ends of the microchannels using a dental sand blaster. After cleaning, the wafer was bonded to a blank fused silica wafer using a reverse RCA[15] procedure and

dx.doi.org/10.1021/ac4014447 | Anal. Chem. 2013, 85, 7133−7138

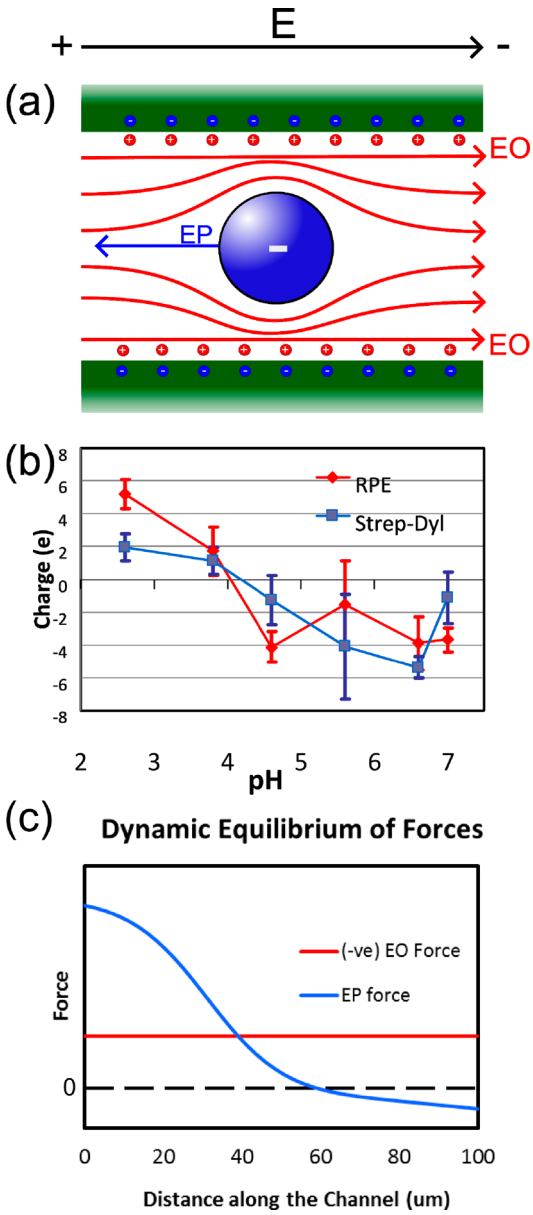

Figure 1. (a) Illustration of the trapping mechanism. Negative fixed charge is blue; positive free charge is red. (b) Zetasizer measurements of the relationship between the protein charge vs pH. The pH and conductivity of the buffers were as follows: pH 2.6 and 1.05 mS/cm; 3.8 and 1.75; 4.6 and 2.51; 5.6 and 3.59; 6.6 and 4.58; 7.0 and 4.87 (c) Illustration of the variation of electro-osmotic (EO) and electrophoretic (EP) forces on an RPE protein along the nanochannel. The electrophoretic force varies with distance along the channel due to the inherent charge−pH relationship of RPE. Focusing occurs at a point along the channel where the sum of EO and EP forces is zero, which is not at the standard PI point.

annealed for 12 h at 1050 °C in air. Wafers were then cut into 7.5 mm wide chips that fit inside a custom-made microscope adapter providing fluid and electrical connections during fluorescence microscopy. The inset in Figure 2 also illustrates a close-up of the nanochannels with a cross-sectional vertical cut made perpendicular to the microchannels for clarity.

Experimental Conditions. Measurements of protein mobility vs pH were made using a Zetasizer (Malvern Instruments). Citric acid buffers of pH values between 2.6 and 7.0 were prepared with the conductivities between 1 and

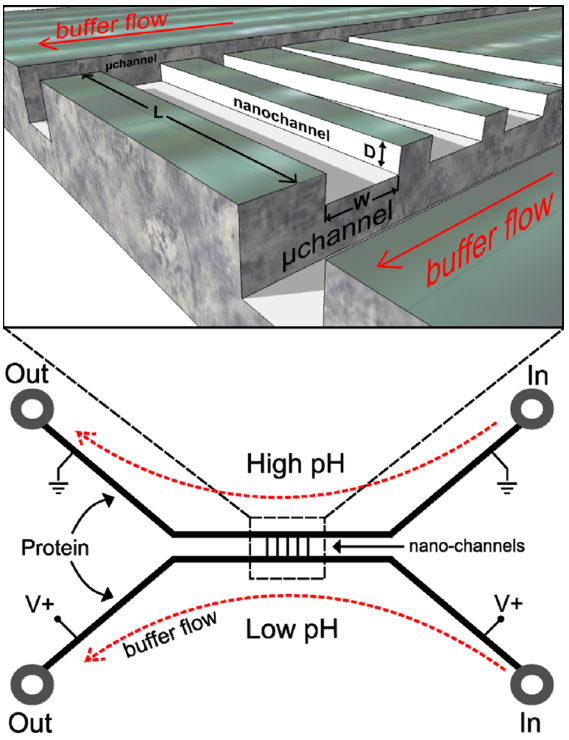

Figure 2. Schematic of the nanochannel device indicating the fluid flow direction (red dotted line) within each microchannel. The inset shows the nanochannels with the top silica layer removed and a vertical slice taken to more clearly illustrate the geometry of the channels. Depth of microchannels is 12.5 ± 0.5 μm. Nanochannels are W = 20 μm wide, L = 100 μm long, and D = 85 ± 5 nm deep.

4.87 mS/cm (details in the description of Figure 1b). It has been shown by Salgin et al.[33] that the variation in conductivity may affect the results of the zeta potential test, but our conductivity span is relatively small and should not affect the general trend of the plot. The buffers were prepared by mixing specific volumes of 0.1 M citric acid solution with 0.2 M disodium orthophosphate (Na_2HPO_4). RPE or Dyl-Strep was added into a buffer at 1.5 mg/mL and measured repeatedly (3 or 4 times). The protein was recovered and resuspended in successive buffers using a 10 kDa cutoff centrifugal. For on-chip focusing, new buffers were created in a similar manner (pH 2.6, 2.7, 3.6, 5.1, 5.8, 6.4, 7.2); however, in order to achieve matching conductivity required to eliminate conductivity gradients along the channel, deionized water and sodium chloride were added until each pH buffer reached 4.60 ± 0.02 mS/cm.

Since protein is stored in a high salt buffer, even a small amount of it added to one buffer could raise the conductivity of one side, producing a conductivity gradient within the nanochannel. Therefore, an equal amount of concentrated protein (RPE or Dyl-Strep) was then added to buffers for both sides of the nanochannel. The final protein concentration of the RPE was 18 μg/mL. The final protein concentration of Dyl-Strep was 50 μg/mL.

During the focusing experiments, each microchannel was continuously supplied with a protein/buffer mixture of different pH values at 1000 nL/min using a Fluigent Fluiwell (France). A regulated power supply was connected to all four fluid ports. Positive electrodes were connected to both ends of the low pH channel, and negative electrodes were connected to both ends of the high pH microchannel. An applied voltage of 0.4 V

dx.doi.org/10.1021/ac4014447 | Anal. Chem. 2013, 85, 7133−7138

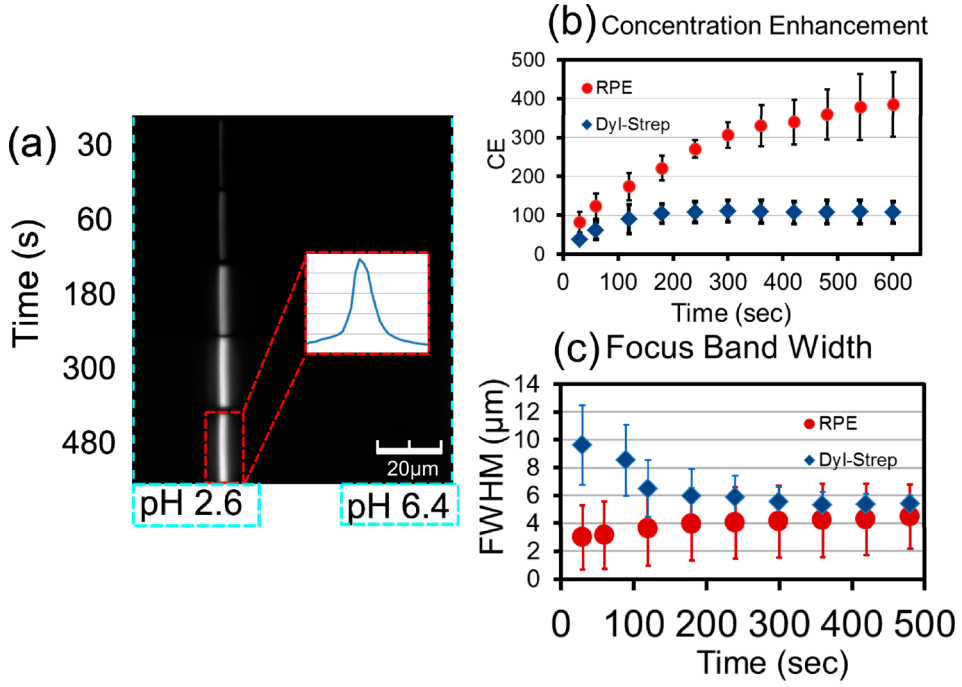

Figure 3. (a) Microscope image time series shows stable and increasing concentration enhancement (CE) of RPE bands. (b) CE versus time of RPE (red dots) and Dyl-Strep (blue diamonds) in separate experiments. (c) Full-width-half-maximum measurement (averaged over 3 trials) approaches approximately 5 μm for both proteins.

typically produced currents of 9.2 ± 0.8 nA. Between experiments, channels were rinsed thoroughly with water and then each reservoir was rinsed with a buffer having a pH and conductivity matching that of the next experiment. Chips were occasionally cleaned by baking in air at 900 °C overnight.

Fluorescence microscopy was used to quantify the focusing of the proteins. A mercury lamp with a standard filter set was used to excite RPE (peak absorption 565 nm, peak emission 573 nm) and Dyl-Strep (peak absorption 488 nm, peak emission 535 nm) within the nanochannel. A Nikon DS-U2 USB camera was used to capture the resulting fluorescence images. As the focus band intensified, the exposure time of the image was decreased to avoid detector saturation. This was later compensated for by using a multiplicative exposure factor during the analyses. The concentration enhancement (CE) factor (to be used henceforth to quantify the protein focusing) is defined as the nanochannel band intensity (I_{Focus}) divided by the high pH microchannel intensity (I_{Micro}) times the microchannel depth (D_{Micro}) divided by the nanochannel depth (D_{Nano}).

$$\mathrm{CE} = \frac{I_{Focus}}{I_{Micro}} \frac{D_{Micro}}{D_{Nano}} \tag{5}$$

RESULTS AND DISCUSSION

Figure 1b shows the results of Zetasizer measurements of protein charge vs pH. The general trend of the plot confirms that, as pH of the buffer increases, the charge of both RPE and Dyl-Strep decreases. Figure 3a shows the concentration of RPE in the nanochannel by pH gradient electrofocusing with a 0.4 V bias applied across the electrodes, positive at the 2.6 pH buffer (left side) and negative at 6.4 pH buffer (right side). A bright focused band of RPE was observed which intensified and maintained a stable position for up to 10 min. Figure 3b,c shows concentration enhancement and bandwidth of RPE and Dyl-Strep using a pH span of 4.2 and a voltage of 0.4 V. RPE reaches an average CE of 385 (Figure 3b) which corresponds to a concentration of 0.028 mM (6.8 mg/mL) at the focus band. Similarly, Dyl-Strep reaches a saturation CE of 107 which corresponds to 0.089 mM (4.8 mg/mL) at the focus. Note that both reach a similar concentration in mg/mL, and so we tentatively attribute the lower intensity of Dyl-Strep to saturation of focusing due to protein precipitation at high concentration focus bands which is common in cIEF.[11]

The nonlinear "saturation" effect observed for the concentration enhancement of both RPE and Dyl-Strep may also be due to photon induced chemical damage (photobleaching) due to the exposure periods required for taking micrographs (<4 s), as well as self-quenching when fluorescent proteins are found in high concentrations. Finally, we note that the observed values of CE for both proteins likely underestimate their true value since the proteins fluoresce less at acidic pH. This pH dependence has not been accounted for in the CE calculations.

Figure 3c shows that RPE and Dyl-Strep bands behaved differently. Dyl-Strep band widths decreased initially while RPE band increased initially, but both approached approximately 5 μm fwhm, which is relatively narrow compared to previously reported experiments with conductivity gradient electrofocusing.[15] Since the concentration of RPE, even in the peak, is still approximately 1000 times lower than the background electrolyte concentration (~30 mM), we do not expect the initial RPE band broadening to be the result of ion substitution by the protein, as in plateau-mode isotachophoresis.[7,8] pH variations across the depth of the nanochannel as described by Bottenus[34] may contribute to the width of the band.

Figure 4 shows that the RPE band depends on the buffer pH present in the reservoirs. The boundaries are kept constant by the continuous flow of buffers running in the microchannels. It is clear that focusing is sharpest when a large pH difference is used. This is indicated by the second band from the top of

dx.doi.org/10.1021/ac4014447 | Anal. Chem. 2013, 85, 7133−7138

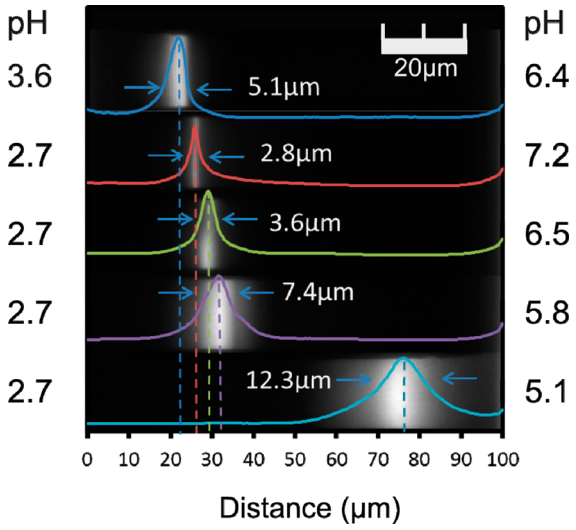

Figure 4. Fluorescence microscopy of RPE focusing using various pH values under 0.4 V bias for 300 s. Note that peak intensities have been normalized. The superimposed line shapes of the focus bands indicate the respective peak widths and position dependence on pH buffer selection. The sharpness measured by the fwhm shows the narrowest band of 2.8 μm results from the widest pH span: 4.2 (pH 2.7 to 7.2). The width of the peaks steadily increases as the pH span is decreased. At the smallest pH span of 2.4 (pH 2.7 to 5.1), the fwhm is 12.3 μm. Note that, when similar buffers were used (close to same pH buffer), no focusing could be observed at all.

Figure 4 which spans 4.5 pH intervals (pH 2.7 to 7.2) and yields a focus band with a fwhm of 2.8 μm. It is also evident that the focus band is broadest when the pH span is smallest; the bottom image of Figure 4 which shows a channel spanning only 2.4 intervals of pH (pH 2.7 to 5.1) yields a focus band fwhm of 12.3 μm. The collection of superimposed plots in Figure 4 suggests that the RPE focuses at a similar pH point regardless of the selected pH boundaries. As pH boundaries are shifted, the focus point moves in a predictable way to where we would expect the focus pH to be located within the new pH gradient.

Figure 5 demonstrates that protein focusing also depended on the voltage applied at the electrodes. Increasing the voltage to 1.2 V generally resulted in a narrower band and faster focusing. The focus band biased at 1.6 V loses some of its uniformity, and above 2 V, the band began to break up. While the intensity continued to increase with voltage, the fluorescent band began to form localized high-intensity points. In addition, the band tended to split apart into multiple bands making the focusing quality inferior. This breakup may be a result of possible precipitation effects due to high concentration of proteins at a sharp focus. Another possible cause of the band break-up is the increasing Peclet number. Higher voltages drive faster convection, which may overcome the ability of the protein to diffusively average the frustrated flow profile leading to leaks in an otherwise stable electrokinetic trap.

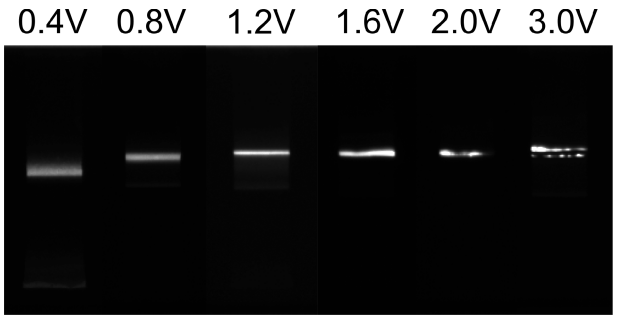

Figure 5. Fluorescence images showing quality of focusing at various bias voltages after 300 s of focusing. RPE focuses into a uniform band at lower voltages below 1.6 V, but at higher voltages, the band becomes distorted and nonuniform. At 3.0 V, the band becomes discontinuous.

We believe that the nanoscale height of the channel is the critical, enabling feature of our method. The small channel depth (85 ± 5 nm) allows protein molecules to diffuse rapidly from top to bottom surfaces, giving a Peclet number of less than unity, effectively averaging the three-dimensional fluid flow velocity and electric field vectors into one dimension where stability is much easier to achieve. Finally, we reiterate that the observed trapping is attributed to pH gradient focusing and unlikely to be the result of electric field gradient trapping due to either nanochannel ion concentration polarization (ICP) or differences in bulk buffer conductivity. The ICP mechanism relies on the selective transport of ions through a nanochannel using identical buffers and produces trapping adjacent to micro−nano interfaces. In this work, we have not observed any trapping in our microchannels or very near the nanochannel ends, nor do we observe any focusing when the two buffers in the microchannels are identical (or very similar). We also emphasize that our buffers had matched bulk conductivity and that trapping is not observed without a significant pH gradient. Further work, especially substantial modeling, is required to more fully understand the interaction of chemical, electrical, and fluid effects that result in this protein focusing phenomena.

■ CONCLUSION

In this work, pH gradient electrofocusing along a nanochannel has been demonstrated for the first time. As an example, RPE and Dyl-Strep were focused using a range of citric acid pH buffers as boundaries of the nanochannel. The optimal quality focus was achieved using a pH span of 2.7−7.2 and a bias voltage of 0.4 V. RPE and Dyl-Strep both approached focus bands widths of around 5 μm with concentration enhancement (CE) factors of 385 and 107, respectively. The technique may be, in principle, capable of achieving multiple protein separation and concentration simultaneously.

■ AUTHOR INFORMATION

Corresponding Author

*E-mail: michael.startsev@mq.edu.au.

Notes

The authors declare no competing financial interest.

■ ACKNOWLEDGMENTS

This work was supported by the Australian Research Council (DP110102207). Microchannel etching was performed at the University of South Australia node of the Australian National Fabrication Facility, established under the NCRIS scheme.

■ REFERENCES

(1) Rose, D. J.; Jorgenson, J. W. *J. Chromatogr., A* **1988**, *438* (0), 23−34.

(2) O'Farrell, P. H. *J. Biol. Chem.* **1975**, *250* (10), 4007−4021.

(3) Regnier, F. E., et al. In *Contemporary Topics in Analytical and Clinical Chemistry*; Springer: New York, 1977; pp 1−48.

(4) Chester, T. L. *Anal. Chem.* **2012**, *85* (2), 579−589.
(5) Grosso, P., et al. *Biomedical Circuits and Systems Conference*. BioCAS 2009. IEEE, 26−28 Nov. 2009; pp 269−272.
(6) El-Aneed, A.; et al. *Appl. Spectrosc. Rev.* **2009**, *44* (3), 210−230.
(7) Persat, A.; et al. *Anal. Chem.* **2009**, *81* (22), 9507−9511.
(8) Garcia-Schwarz, G.; et al. *J. Vis. Exp.* **2012**, *61*, No. e3890.
(9) Strychalski, E. A.; et al. *Anal. Chem.* **2009**, *81* (24), 10201−10207.
(10) Ross, D. *Electrophoresis* **2010**, *31* (22), 3650−3657.
(11) Pritchett, T. J. *Electrophoresis* **1996**, *17* (7), 1195−1201.
(12) Kim, S. J.; et al. *Chem. Soc. Rev.* **2010**, *39* (3), 912−922.
(13) Wang, Y.-C.; et al. *Anal. Chem.* **2005**, *77* (14), 4293−4299.
(14) Zangle, T. A.; et al. *Chem. Soc. Rev.* **2010**, *39* (3), 1014−1035.
(15) Inglis, D. W.; et al. *Angew. Chem., Int. Ed.* **2011**, *50* (33), 7546−7550.
(16) O'Farrell, P. H. *Science* **1985**, *227* (4694), 1586−1589.
(17) Raj, C. *J. Biochem. Biophys. Methods* **1994**, *3*, 161−172.
(18) Koegler, W. S.; Ivory, C. F. *J. Chromatogr., A* **1996**, *726* (1−2), 229−236.
(19) Hlushkou, D.; et al. *Lab Chip* **2009**, *9* (13), 1903−1913.
(20) Huang, Z.; Ivory, C. F. *Anal. Chem.* **1999**, *71* (8), 1628−1632.
(21) Ross, D.; Locascio, L. E. *Anal. Chem.* **2002**, *74* (11), 2556−2564.
(22) Tang, G.; Yang, C. Temperature Gradient Focusing. In *Encyclopedia of Microfluidics and Nanofluidics*; Springer-Verlag: Berlin, Heidelberg, 2008.
(23) Kolin, A. *J. Chem. Phys.* **1954**, *22* (9), 1628−1629.
(24) Righetti, P. G. *Immobilized pH gradients: theory and methodology*; Elsevier Science Publishers B.V. (Biomedical Division): Amsterdam, 1990.
(25) Chingin, K.; et al. *Anal. Chem.* **2012**, *84*, 6856−6862.
(26) Millioni, R.; et al. *PLoS One* **2011**, *6* (5), No. e19603.
(27) Polaskova, V.; et al. *Electrophoresis* **2010**, *31* (3), 471−482.
(28) Vazquez, M.; et al. *Analytical chemistry* **2002**, *74* (9), 1952−1961.
(29) Tandon, V.; et al. *Electrophoresis* **2008**, *29* (5), 1092−1101.
(30) Chang, H.-C.; Yeo, L. *Electrokinetically Driven Microfluidics and Nanofluidics*; Cambridge University Press: New York, 2010.
(31) Berthier, J.; Silberzan, P. *Microfluidics for Biotechnology*, 2nd ed.; Artech House: Norwood, MA, 2006; p 483.
(32) Berg, H. C. *Random Walks in Biology*; Princeton University Press: Chichester, 1993; p 194.
(33) Salgin, S.; et al. *Int. J. Electrochem. Sci.* **2012**, *7*, 12415−12431.
(34) Bottenus, D.; et al. *Lab Chip* **2009**, *9* (2), 219−231.